Study of Self-Diffusion of Hyperbranched Polyglycidols in Poly(vinyl alcohol) Solutions and Gels by Pulsed-Field Gradient NMR Spectroscopy

W. E. Baille and X. X. Zhu*

Département de Chimie, Université de Montréal, C.P. 6128, Succ. Centre-ville, Montréal, Québec H3C 3J, Canada

S. Fomine

Instituto de Investigaciones en Materiales, Universidad Nacional Autónoma de México, Apartado Postal 70-360, CU, Coyoacán, México DF04510, México

Received March 1, 2004; Revised Manuscript Received August 29, 2004

ABSTRACT: In an effort to further understand the effects of molecular size and shape of macromolecular diffusants on the diffusion in hydrophilic polymer solutions and gels, hyperbranched polyglycidols have been synthesized as hydrophilic diffusants and characterized. Four of these hyperbranched polymers were selected for the study of self-diffusion by pulsed-field gradient NMR spectroscopy in poly(vinyl alcohol)−water systems. The effects of the molecular weight, size, and shape of the diffusant, polymer concentration, and temperature have been studied. For diffusants of similar molecular weight and without specific interactions, the activation energy decreases from the dendrimers to hyperbranched polymers and then to linear polymers. The results indicate that the molecular shape, and hence the molecular density distribution of the diffusants, is important in the diffusion process.

Introduction

The molecular diffusion in polymer matrices has been studied by different techniques. Examples include cooperative diffusion of globular protein in solution by dynamic light scattering,[1] probe diffusion by Taylor dispersion and phosphorescence quenching,[2] drug release from polymer gels by gravimetric measurements,[3] and solute diffusion in hydrogels by pulsed field gradient (PFG) NMR techniques.[4] The results of these studies helped in the understanding of the diffusion phenomena in polymer systems. The effects of polymer concentration, size, and shape of the diffusant, temperature, and specific interactions within the polymer matrix are all important in determining the diffusion properties in a polymer system, which ultimately determines the applicability of polymeric materials in industry. Also, the data allowed to develop and to test over the years various physical models of diffusion.[5−13] The physical models of diffusion are essential for the interpretation of the results.

The molecular size and shape of the diffusants are known to have an effect on the diffusion of plasticizers in poly(vinyl chloride)[14−16] and in epoxy resins during curing[17] and in poly(methyl methacrylate).[18,19] We have studied the self-diffusion of solute molecules ranging from small molecules to polymers and from linear to more spherical molecules in polymer solutions and gels[11,20−24] in an effort to elucidate the effects of functional groups (alcohol, amine, ammonium salt, amide and acid),[11,20] diffusant size and shape, polymer concentration, and temperature in the diffusion process.[21−24] Recently, our study showed the difference in the activation energy between poly(propylenimine) (PPI) dendrimers with hydrophilic triethylenoxy methyl ether (TEO) terminal groups and linear poly(ethylene glycol)s (PEGs) of comparable molecular weights.[24] The results show that the self-diffusion coefficient is greater for the dendrimers than the linear PEGs when the molecular weights and experimental conditions are similar. The same trend was observed for various polymer concentrations.

To obtain a better understanding of the shape effect on the self-diffusion of the molecules and to put the model of Petit et al. on a more rigorous footing, we have made four hyperbranched polygycidols and studied their self-diffusion in poly(vinyl alcohol) (PVA) solutions and gels by PFG NMR spectroscopy. These molecules can be considered to possess intermediate shapes between linear polymers and more spherical dendrimers. Therefore, a comparison is also made with previous data obtained with linear PEGs and dendrimers.

Experimental Section

Materials. Glycidol (96%), dioxane, potassium methoxide (95%), and all other chemicals were purchased from Aldrich (Milwaukee, WI). D_2O was purchased from C.I.L. (Andover, MA). All chemicals were used as received.

Preparation of Hyperbranched Polyglycidol (HBPG).[25,26] Glycidol (50 g, 675 mmol) was added dropwise under a nitrogen flow for 12 h at 90 °C into a suspension of potassium methoxide (0.25 g, 3.5 mmol) in dioxane (50 mL). When the reaction was completed, dioxane was removed under vacuum, and polyglycidol was obtained as very viscous syrup. The polymer was neutralized with concentrated HCl.

HBPG was fractionated on a preparative size exclusion chromatography system equipped with two columns (Shodex OHpak SB-2003 and -2004). The flow rate of the eluent was at 2.0 mL/min. The columns and the detector were equilibrated at 33 and 35 °C, respectively.

Size Exclusion Chromatography (SEC). The molecular weight of selected polymer fractions was measured on a SEC system equipped with a Waters 1525 binary HPLC pump, a Waters 2410 refractive index detector, and a set of three Ultrahydrogel columns (Ultrahydrogel 120, 500, and 2000). Poly(ethylene glycol) (PEG) and poly(ethylene oxide) (PEO) were used as standards for the calibration. The polymers were dissolved in water at a concentration of 2 mg/mL and filtered

* To whom correspondence should be addressed: e-mail julian.zhu@umontreal.ca.

10.1021/ma049588a CCC: $27.50
Published on Web 10/19/2004

through 0.45 μm filters before injection. The flow rate of the eluent was at 0.5 mL/min. The columns and the detector were equilibrated at 33 and 35 °C, respectively.

NMR Spectroscopy. ^{1}H NMR, inverse gated ^{13}C NMR, and DEPT-135 (distortionless enhancement by polarization transfer) experiments of the polymer samples in DMSO-d_6 and D_2O (with a small amount of copper sulfate as relaxation agent) were performed on a Bruker AV-400 spectrometer operating at a frequency of 400.13 MHz for ^{1}H and 100.63 MHz for ^{13}C to characterize the hyperbranched polyglycidols.

MALDI−TOF Mass Spectrometry. The molecular weight of all samples was also measured by using a Kratos Kompact MALDI-III TOF mass spectrometer benchtop model. The system generates a maximum laser out of 6 mW at a wavelength of 337 nm (N_2 laser light, 3 ns pulse width). All the samples in this study were analyzed by using the reflection mode to obtain a higher mass resolution. α-Cyanohydroxycinnamic acid was used as the matrix. Before the molecular weight measurement, samples were prepared by dissolving the hyperbranched polymers in water at a concentration of 5 mg/mL. Into this solution, 10 mg/mL of the matrix aqueous solution and 5 mg/mL of LiBr aqueous solution were added. 0.1 μL of this mixture was applied to a spot on a sample slide, and the solvent was allowed to evaporate slowly to create a thin matrix−analyte film.[27]

Pulsed Field Gradient NMR Measurements. To measure the self-diffusion coefficient (D), samples were prepared following the method described previously.[11,21] PVA (M_n = 52 000 with a degree of hydrolysis equal to 99%) was added to a D_2O solution containing 1 wt % of diffusant in 5 mm o.d. NMR tubes. The concentration of PVA ranged from 0 to 0.32 g/mL.

D values were determined using the stimulated echo (STE: 90°−t_1−90°−t_2−90°−t_1−echo) technique developed by Tanner[28] on a Bruker DSX-300 NMR spectrometer operating at a frequency of 300.18 MHz for protons. Details on the NMR experiments were described previously.[24] The self-diffusion coefficients were extracted by using the following expression[29−31]

$$\ln \frac{I}{I_0} = -\frac{t_2}{T_1} - \frac{2t_1}{T_2} - \ln 2 - \gamma^2\delta^2G^2D(\Delta - \delta/3) \qquad (1)$$

where I and I_0 are the NMR signal intensities in the presence and in the absence of the gradient and the relaxation processes, respectively, t_1 is the interval between the first two 90° rf pulses and between the third 90° rf pulse and the middle of the echo, t_2 is the delay between the second and the third 90° rf pulses, γ is the gyromagnetic ratio of the nucleus under observation, T_1 and T_2 are the spin−lattice and the spin−spin relaxation times, respectively, δ and G are the duration and the strength of the applied gradient pulse, respectively, D is the self-diffusion coefficient, and Δ is the time interval between the two successive gradient pulses (also called the diffusion time). The self-diffusion coefficient was extracted from the slopes of the lines obtained from linear regression of the logarithm of signal intensity as a function of G^2. Excellent linear relationships have been obtained in these experiments with correlation coefficients of 0.985 and better. The error of the measured D values was estimated to be ≤7% by carrying out repeated experiments with selected samples. The accuracy of results can be determined by studying samples with known self-diffusion coefficients such as pure water and pure glycerol, and good agreement was obtained at 25 °C with values reported in the literature.[32,33]

The experiments were performed at different temperatures for all HBPG samples at 25, 35, 45, and 55 °C (fluctuation of the temperature ±0.3 °C), and concentrations of PVA ranged from 0 to 0.32 g/mL. Temperature calibration was done periodically on the NMR instrument by measuring the chemical shift difference between the ^{1}H NMR signals of CH_2 and OH groups of pure ethylene glycol at various temperatures since this difference is sensitive to temperature changes.[34]

A nonlinear least-squares fitting method was used in all cases to fit the experimental diffusion data to the model of Petit et al.[11] The correlation coefficients r^2 yielded were in the range 0.989−0.999. The quality of the fitting to the experimental data was also indicated by the good fits shown in all the figures. The same sets of fitting parameters were obtained regardless of the initial values used in the procedure.

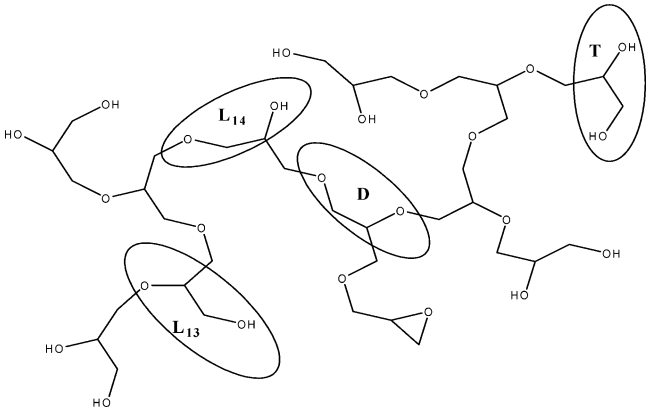

Figure 1. Schematic structure of the hyperbranched polyglycidol. Examples of the dendritic segment (D_s), linear 1,3-segment (L_{s13}), linear 1,4-segment (L_{s14}), and terminal segment (T_s) as indicated by concentric lines.

Table 1. Determination of the Molecular Weights of HBPGs by SEC and MALDI−TOF Mass Spectrometry

	SEC		MALDI-TOF	
samples	M_n[a]	M_w/M_n[b]	M_n[a]	M_w/M_n[b]
HBPG-1	226	1.14	324	1.81
HBPG-2	672	1.48	629	1.18
HBPG-3	1890	1.26	1102	1.44
HBPG-4	3245	1.19	1868	1.02

[a] Number-average molecular weight. [b] Polydispersity.

Results and Discussion

Characterization of Hyperbranched Polyglycidols. From glycidol monomers, HBPGs have been synthesized by ring-opening polymerization initiated with potassium methoxide. During the initiation a primary alkoxide and a secondary alkoxide can be formed. In the propagation step, these two alkoxide species can both react with glycidol. The structure of resulting polymers is shown in Figure 1. Both intermolecular and intramolecular chain transfers can take place.[26] Macrocyclic products may also be formed[26] if the primary alkoxide reacts with the epoxy group from glycidol monomer. When the reaction is completed, a light yellow viscous liquid is obtained.

The number-average molecular weight (M_n) of the product determined by SEC was ca. 3000 g/mol with a polydispersity of 2.9. The HBPG was then fractioned by preparative SEC. The molecular weight and the polydispersity obtained by SEC for four selected fractions are listed in Table 1. However, these molecular weights are only relative to the linear PEG and PEO used as standards. To obtain a basis of comparison of the molecular weights, MALDI−TOF mass spectrometry was also used for the characterization. The number-average molecular weights obtained for samples HBPG-1 and HBPG-2 by the MALDI−TOF technique are in good agreement with the SEC results (Table 1). For HBPG-3 and HBPG-4, the degrees of branching (DB) (see Table 2 and the discussion below) are higher and the differences of M_n obtained with the two analytical methods are larger. The deviation of the SEC results for HBPG-3 and HBPG-4 may result from the use of linear PEGs as standards in the measurements of

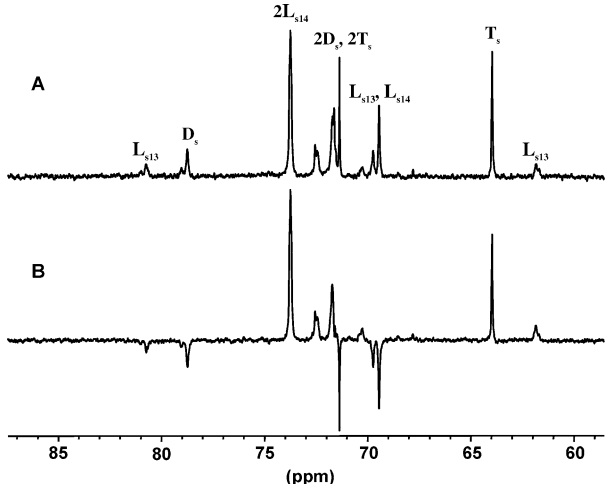

Figure 2. ^{13}C NMR spectrum (A) and DEPT-135 NMR spectrum (B) obtained for HBPG-1 in DMSO-d_6. D_s corresponds to the dendritic segment of the HBPG, and L_{s13} and L_{s14} symbolize respectively the linear 1,3-segment and the linear 1,4-segment. T_s represents the terminal segment of HBPGs.

Table 2. Relative Abundance of Substructure Units and Degree of Branching (DB) of HBPGs Obtained by Inverse Gated^{13}C NMR Spectroscopy

	relative abundance (%)				
samples	dendritic (D_s)	linear 1,3 (L_{s13})	linear 1,4 (L_{s14})	terminal (T_s)	DB
HBPG-1	7	4	34	55	0.28
HBPG-2	12	14	38	36	0.32
HBPG-3	16	14	35	35	0.40
HbPG-4	19	17	34	30	0.43

hyperbranched polymers. The M_n and the polydispersity obtained by MALDI−TOF are used in the analysis of the results in this study since we consider that these values are not affected by the choice of calibration standards as in SEC. Even so, the ion formation in the MALDI−TOF method may result in the breaking up of the polyglycidol chains which may yield lower M_n than the real values, especially when the reflectron mode is used.[35]

Quantitative inverse gated ^{13}C NMR spectra and DEPT-135 spectra of the polymers are used to identify the structure of each HBPG fraction. Figure 2 shows the ^{13}C NMR and DEPT-135 spectra obtained for sample HBPG-1. All signals have been assigned by Tokar et al.[36] and Sunder et al.,[26] D_s corresponds to the dendritic segment, L_s symbolizes the linear segment, and T_s represents the terminal segment of HBPG. The linear segment may be composed of either a linear 1,3-unit (L_{s13}) or a linear 1,4-unit (L_{s14}). A L_{s13} segment is obtained when the secondary hydroxyl group has propagated. A L_{s14} segment is obtained when the primary hydroxyl has propagated. Table 2 shows the relative abundance in percentage determined from the relative integrals of the inverse gated ^{13}C NMR signals for each segment of the HBPG. Apparently, the relative abundance of the segment L_{s13} increases with the molecular weight. However, the segment L_{s14} does not depend on the molecular weight. Nevertheless, the D_s part increases with the molecular weight while the T_s part decreases. Table 2 also shows that the relative abundance of segment L_{s14} is always at least twice higher than segment L_{s13} since the primary alkoxide has a lower sterical hindrance and a higher stability than the secondary alkoxide.[26,37] This combination makes the primary alkoxide more reactive than the secondary alkoxide. From the relative abundance values in Table 2, the DB has been estimated for each fraction by the general definition of DB for an AB_2 system:[26,38,39]

$$\mathrm{DB} = \frac{2D_s}{2D_s + L_{s13} + L_{s14}} \qquad (2)$$

The degree of branching measures the suitability of a hyperbranching reaction to create dendritic structure. Thus, for a linear polymer, the DB is 0. For a homopolymerization of AB_2 monomers, the DB is 0.5 when the two B groups have the same reactivity during a random polymerization. In the case of a perfect dendritic polymer, the DB is 1. Table 2 shows the DB obtained for each fraction. The values obtained are between 0.28 and 0.43. This result indicates that the addition of glycidol during the reaction was fast since an ideal slow addition gives a DB of 0.66.[26] However, the value of DB increases with the molecular weight as expected.[39]

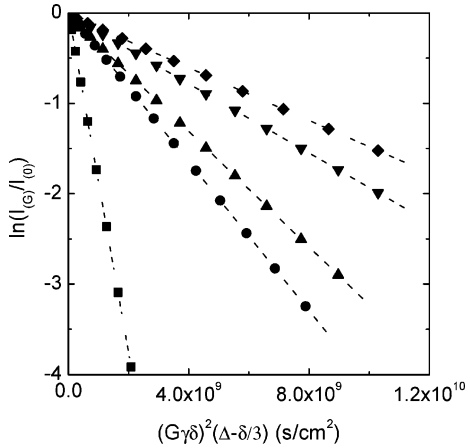

Figure 3. Semilogarithmic plot of the attenuation of the HBPG NMR signals in a 1 wt % aqueous solution (without PVA) at 25 °C as a function of $(G\gamma\delta)^2(\Delta - \delta/3)$, where δ is fixed to a value between 0.7 and 1.0 ms and $\Delta = 400$ ms. Squares, HOD; circles, HBPG-1; up triangles, HBPG-2; down triangles, HBPG-3; diamonds, HBPG-4.

Diffusion Measurements. Figure 3 shows a semilogarithmic of the NMR signal attenuations as a function of $\gamma^2\delta^2G^2(\Delta - \delta/3)$, where δ was fixed to a value between 0.7 and 1.0 ms and Δ was set to 400 ms. From eq 1, we know that this relationship is linear when the diffusion is isotropic and the slope of the line equals $-D$. The self-diffusion coefficient was determined on all directions (x, y, and z) of the applied gradient pulse. For each axis, values obtained are identical within the estimated experimental error (error is less than 7%), indicating the diffusion is isotropic. Attempts also were made to detect possible restricted diffusion of the HBPG by measuring their self-diffusion coefficient as a function of Δ from 20 to 600 ms for the HBPG with three different PVA concentrations (0.03, 0.12, and 0.32 g/mL), and the self-diffusion coefficients obtained are identical. Therefore, no restricted diffusion is present. Thus, the good linearity shown in Figure 3 indicates that the self-diffusion coefficients are monoexponential and the D values obtained decrease from HOD to HBPG-4. The concentration of the diffusant was always set at 1 wt %, low enough to minimize interactions between diffusant molecules during the diffusion process. Thus, the self-diffusion coefficient obtained represents clearly the influence of the effective size (or the molecular weight)

Table 3. Experimental Self-Diffusion Coefficients (D_0), Hydrodynamic Radii (R_h), and Fitting Parameters $k\beta^2$ and D_0 Obtained for the HBPG in Aqueous PVA Systems

samples	R_h[a] (nm)	D_0 (10^{-10} m^2/s) exptl	D_0 (10^{-10} m^2/s) calcd[b]	$k\beta^2$[a] (10^{-10})	R^2[c]
HBPG-1	0.48	4.12 ± 0.01	4.10 ± 0.05	0.29 ± 0.02	0.999
HBPG-2	0.62	3.19 ± 0.01	3.17 ± 0.04	0.18 ± 0.01	0.998
HBPG-3	1.04	1.92 ± 0.01	1.87 ± 0.05	0.10 ± 0.01	0.991
HBPG-4	1.37	1.46 ± 0.01	1.43 ± 0.04	0.07 ± 0.01	0.993

[a] Calculated from eq 3. [b] Obtained as a fitting parameter from eq 5 when the average value of ν is used (0.58). [c] Root-mean-square errors of the nonlinear least-squares fitting to eq 5.

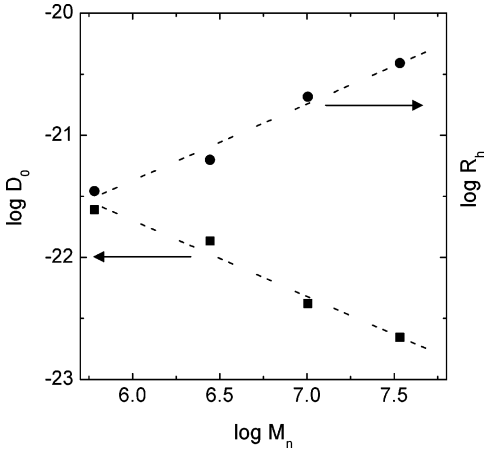

Figure 4. Dependence of D_0 and R_h of HBPGs on their molecular weights at 25 °C.

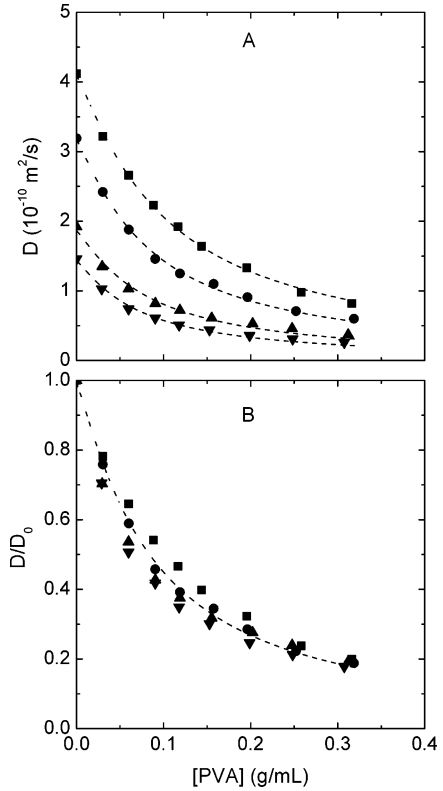

Figure 5. (A) HBPG self-diffusion coefficients as a function of PVA concentration at 25 °C. (B) Normalized self-diffusion coefficients (D/D_0) of the HBPG diffusants as a function of PVA concentration. Dashed lines are fits to eq 6. Squares, HBPG-1; circles, HBPG-2; up triangles, HBPG-3; down triangles, HBPG-4.

on the self-diffusion coefficient. This affirmation is correct only if the magnitude of the specific interactions between the diffusant and the solvent is similar for all HBPG molecules. The decrease in D values with the effective size (or the molecular weight) can be described by the Stokes−Einstein equation if HBPG molecules can be considered as an uncharged spherical particle at infinite dilution moving in laminar flow:

$$D = \frac{k_B T}{6\pi\eta R_h} \tag{3}$$

where D is the self-diffusion coefficient, k_B the Boltzmann constant, T the absolute temperature, η the viscosity of the solvent (D_2O), and R_h the effective hydrodynamic radius of the diffusing molecule, which is related to $\bar{\nu}$ (the partial specific volume) and M (the molecular weight) of the diffusant by the following equation:[40]

$$R_h = \sqrt[3]{\frac{3M\bar{\nu}}{4\pi N}} \tag{4}$$

The combination of eqs 3 and 4 shows clearly that when the shape of the diffusant is spherical and without any specific interactions between the diffusant and the solvent, the self-diffusion coefficient must be inversely proportional to the cubic root of the diffusant molecular weight. To verify qualitatively the shape of HBPG molecules, the self-diffusion coefficient in the absence of any polymer (D_0) and the effective size (R_h) deduced from eq 3 (Table 3) were plotted as a function of the molecular weight. Figure 4 shows logarithmic plots of D_0 and R_h vs the molecular weight. The values of the slope obtained for both variations are identical but have opposite signs (slope = 0.62). The resulting slope value for HBPG molecules shows clearly that these molecules are not spherical in shape, since a slope value of 0.33 is expected for a spherical diffusant as illustrated by eq 4.

Qualitative evaluation of the density distribution (or the fractal dimension) of polymers can be also deduced from Figure 4. The slope value obtained corresponds to the Flory exponent (α), which provides qualitative information on the polymer conformation in dilutes solutions.[24,41−44] The value obtained for HBPG diffusants indicates that the density distribution of HBPGs is similar to that of a swollen polymer chain or polymer in a good solvent.[44−48] Thus, the fractal dimension value (1/α) is equal to 1.62, which indicates that the HBPGs conformation is like an expanded coil. According to Stancik et al.[46] and King et al.,[49] randomly branched polymers are characterized by 1/α = 2 in a good solvent or 1/α = 2.28 in a θ-solvent. The 1/α value of HBPG may be a further indication of their relatively lower degree of branching as shown in Table 2.[50] In comparison to the previous results obtained for PPI$(TEO)_x$ dendrimers (slope = 0.40 and 1/α = 2.5) and linear PEGs (slope = 0.49 and 1/α = 2.0), it is clear that the density distributions for the three kinds of diffusants are different. In the case of linear PEG, 1/α corresponds to polymer coils in a θ-solvent.[48] For the PPI$(TEO)_x$ dendrimers, the fractal dimension value is smaller than the expected value (slope = 0.33 and 1/α = 3 for a diffusant with a perfect spherical shape), indicating a compact space-filling structure.[44]

(1) Effect of Polymer Concentration. Figure 5A shows a plot of self-diffusion coefficients of HBPG as a function of PVA concentration. As obtained in previous studies in PVA,[11,21,23,24] the D values decrease with the

PVA concentration, from 0 to 0.32 g/mL. This concentration range covers the dilute to the viscous gel regimes. We assume that at the dilute regime the decrease of the self-diffusion coefficient is principally influenced by the viscosity of the PVA solutions. However, the decrease in the D between the semidilute and the viscous gel regimes is greatly influenced by the capability of the polymer chain to form a network at the concentration. By analogy to de Genne's scaling laws, this network can be characterized by a correlation length, ξ.[51] According to these scaling laws[51] and from the description of solute diffusion in hydrophilic networks by Peppas et al.,[52] ξ should decrease rapidly while the polymer concentration increases. This decrease of ξ with the polymer concentration is a result of contacts and entanglements of the polymers. Thus, the increased contacts and entanglements induce greater difficulties for the diffusant to pass through the polymer matrix. However, in the viscous gel regime, the ξ decreases more slowly. Thus, the effect of the polymer concentration on the self-diffusion coefficient tends to be less significant, as illustrated in Figure 5A.

Figure 5A also shows a dependence of the self-diffusion coefficients on the molecular weight or the effective size of the diffusant. However, this molecular weight effect becomes less significant for HBPG with higher molecular weights. The same results have been obtained previously for linear poly(ethylene glycol) and hydrophilic dendrimer diffusants.[11,21,23,24] Dashed lines in Figure 5A represent the result of the fit to the model of Petit et al. as shown in the following equation[11]

$$D = \frac{D_0}{1 + ac^{2\nu}} \tag{5}$$

where $a = D_0/k\beta^2$ and k represents the jump frequency over the energy barriers, which is expected to depend on the size of the diffusant and on the specific interactions between the diffusant and the polymer matrix. The k parameter depends also on the temperature. This jump frequency can be written in an Arrhenius form:

$$k = F_{\mathrm{p}} \exp\left(\frac{-\Delta E}{k_{\mathrm{B}}T}\right) \tag{6}$$

where F_{p} is a frequency prefactor and ΔE is the height of the potential barrier.

The model was used to fit the variation of the self-diffusion coefficient as a function of PVA concentration for all HBPGs. If we allow all parameters (D_0, $k\beta^2$, and ν) to vary, ν ranges from 0.48 to 0.58 for HBPGs. For all the fits obtained, the average value of ν in this work and in previous studies was used.[21,22] This average value ($\nu = 0.58$) is approximately equal to the value expected for the case of a marginal solvent ($\nu = 0.50$).[53]

Schaefer and Han have shown that in the semidilute regime the exponent ν value obtained from the proportionality equation between the polymer cooperative diffusion constant (D_{c}) and the monomer volume fraction (φ) is 0.75 for a good solvent, 0.5 for a marginal solvent, and 1.0 for poor solvent.[53] The values of this exponent as an indication of the quality of the solvent are essentially the same as those of the Mark−Houwink parameter α in the relation $R_{\mathrm{g}} = KM_{\mathrm{w}}^{\alpha}$. Different results for PVA−water systems have been found in the literature. For example, Horkay et al. obtained an exponent value 0.77 by dynamic light scattering for PVA concentrations higher than 0.10 g/mL,[54] corresponding to a good solvent. However, Flory's interaction parameter obtained by the same authors ($\chi = 0.484$) is close to the expected value for a θ-system ($\chi = 0.5$).[54] Nevertheless, this value ($\chi = 0.484$) indicates that water is a marginal solvent for the range of PVA concentrations used by Horkay et al.[54] On the other hand, results obtained by Wang et al. yielded a value of 0.56 for the exponent α for the PVA−water solutions[55] while a recalculation of the data[56] provides a value of 0.71. These values correspond to the values expected for random coils in a θ-solvent ($\alpha = 0.5$) and for polymers in a good solvent ($\alpha = 0.75$), respectively.

According to de Gennes, a transition from good solvent to poor solvent occurs at $\Phi = 1 - 2\chi$, where Φ is the fraction of sites occupied by monomers if the polymer solution is taking as a periodic lattice and χ represents the interaction parameter of Flory.[51] Using this relation, the transition from good to poor solvent should occur at a PVA concentration of 0.012 g/mL with $\chi = 0.484$.[54,57] This indicates that the concentration range of PVA used in this study should correspond to the situation of a poor solvent. However, the PVA−D_2O samples were homogeneous as indicated by the clear solutions so that the solvent should not be a poor one though it can be a marginal one (as indicated by the measured ν values). The thermal history of a PVA solution can be important,[58] since the clear PVA solution may become opaque over time and becomes clear again when heated. The values of the parameters D_0 and $k\beta^2$ obtained from the fit with eq 5 are listed in Table 3. It shows that excellent agreement of the D_0 values obtained from fitting to the ones measured by the NMR experiments. This comparison is a good indication of the data quality, and the difference is well within the margin of errors obtained (less than 15% for the parameters obtained from the fit with the model of Petit et al.). The D_0 values in the table decrease with the molecular weight. This result agrees well with eq 3, which relates the self-diffusion coefficient to the inverse of the cubic root of the molecular weight. The $k\beta^2$ parameter observed for all samples in Table 3 decreases when the molecular weight (or size) of HBPG increases. The same decrease has been observed in previous works.[11,21,23,24] Since β remains constant for a given polymer−solvent system,[11] the results shown in Table 3 confirm that an increase in the molecular size leads to a lower jump frequency. Thus, the higher the molecular weight of the diffusant is the more difficult it would be for the diffusant to diffuse in the polymer matrix.

Figure 5A shows the effects of molecular weights of the diffusants and of PVA concentration on the self-diffusion coefficient of HBPGs. However, to obtain insight into the effect of specific chemical interactions between HBPG and PVA matrix, we choose to normalize the self-diffusion coefficients (D/D_0) and plot them as a function of PVA concentration. Figure 5B shows this normalized diffusion coefficients (D/D_0) of HBPG with different molecular weights as a function of PVA concentration. The first look of Figure 5B shows that the data points of all diffusants follow the same trend. Indeed, the beginning of the curves starts at the same point and the ends of the curves also seem to converge to similar values. A closer examination of the curves reveals that in the middle section the D/D_0 values of the different diffusants vary significantly. This indicates that the effect of interactions with the polymer network

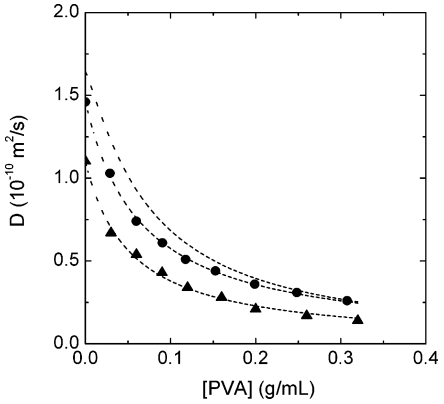

Figure 6. Variation of the self-diffusion coefficients of various diffusants as a function of PVA concentration. All diffusants have similar molecular weight (2000 g/mol) but different shapes. Dashed lines are fits to eq 5. Squares, poly(propylenimine) dendrimers; circles, HBPG-4; triangles, linear PEG.

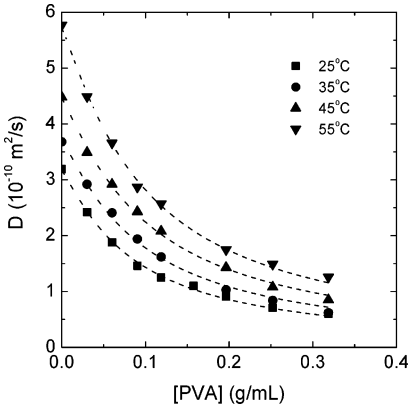

Figure 7. Self-diffusion coefficients of the HBPG-2 as a function of PVA concentration at four different temperatures. Dashed lines are fits to eq 5.

have an effect in the intermediate concentration range of PVA. Within this concentration range a screening effect becomes possible.

To study the effect of the shape of the diffusants on the self-diffusion coefficient, comparison can be made among HBPGs, PPI(TEO)$_x$ dendrimers, and linear poly(ethylene glycol)s with similar molecular weights around 2000 g/mol. The variation of the self-diffusion coefficient with the diffusant shape is shown in Figure 6, and the self-diffusion coefficients of the dendrimer are systematically higher than those of the HBPG. At higher PVA concentrations, the two kinds of diffusants tend to converge to similar D values. Figure 6 also shows that the self-diffusion coefficients of the HBPG are always higher than those of the linear PEG. The more spherical shape of the dendrimer makes it easier to diffuse in the polymer matrix than the linear PEG of the same molecular weight. Obviously, for the same PVA concentration (or the same mesh size of the transient statistical network), it is easier for a dendrimer to overcome the energy barrier to diffuse in the network. HBPG has a molecular shape between a more spherical dendrimer and a linear polymer. In the absence of specific interactions, the self-diffusion coefficients of the HBPG lie between those of a dendrimer and of a linear polymer as shown in Figure 6. The size and shape of the diffusants determine the self-diffusion process of these molecules.

(2) Effect of Temperature. The self-diffusion coefficients of the HBPGs were determined over a temperature range from 25 to 55 °C for eight or nine different PVA concentrations (from 0 to 0.32 g/mL). An example (HBPG-2) of the results is shown in Figure 7. In general, D increases with increasing temperature, but the effect of temperature becomes less significant with increasing PVA concentration. This result indicates that at higher PVA concentration the network is less affected by the temperature. The same behavior (i.e., the reduction of the temperature effect on the self-diffusion coefficient at higher PVA concentrations) was observed for the three other hyperbranched polymers (HBPG-1, HBPG-2, and HBPG-4, data not shown). Furthermore, the effect of the temperature on the self-diffusion coefficient is less significant with increasing molecular weight (data not shown). These results agree well with the one obtained for PPI(TEO)$_x$ dendrimer in a previous study.[24] Dashed lines illustrated in Figure 7 are the result of the fit with the model of Petit et al. (eq 5), and these fits show good agreement between the model and the experimental data. The $k\beta^2$ parameters obtained from the fit observed at each temperature are used to determine the apparent activation energies (E_a) for each HBPG as illustrated in Figure 8. This E_a has been determined using an equation similar to eq 6, conveniently represented by ΔE. Since the constant β is unknown, $k\beta^2$ is kept as the variable, reflecting the variation of k as a function of temperature.

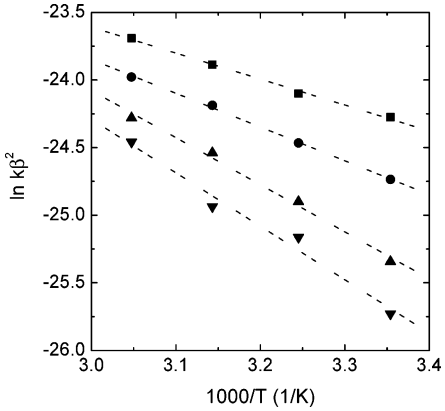

Figure 8. Semilogarithmic plot of the $k\beta^2$ parameter as a function of reciprocal temperature for HBPG diffusants: squares, HBPG-1; circles, HBPG-2; up triangles, HBPG-3; down triangles, HBPG-4.

Figure 9A shows the variation of the E_a obtained from the Arrhenius approach with molecular weight of the HBPG. As expected, the apparent activation energy increases with the molecular weight. Figure 9A also shows the same trend for PPI(TEO)$_x$ dendrimers and the linear PEGs. However, for a similar molecular weight, the E_a values of PPI(TEO)$_x$ dendrimers, HBPGs, and linear PEGs increase from the dendrimers to the linear PEGs. This trend confirms the results in Figure 6 which show that when the diffusion process is not under the control of specific interactions and for the diffusants with similar molecular weights, the effect of molecular size (derived from the shape of the molecules) is the most important on the diffusion process. To illustrate more clearly this effect, Figure 9B shows a plot of E_a as a function of the ratio of R_h/M_n. It is interesting to observe in that E_a varies almost linearly with R_h/M_n for the three types of diffusants. The ratio of R_h/M_n can be regarded as an indication of specific

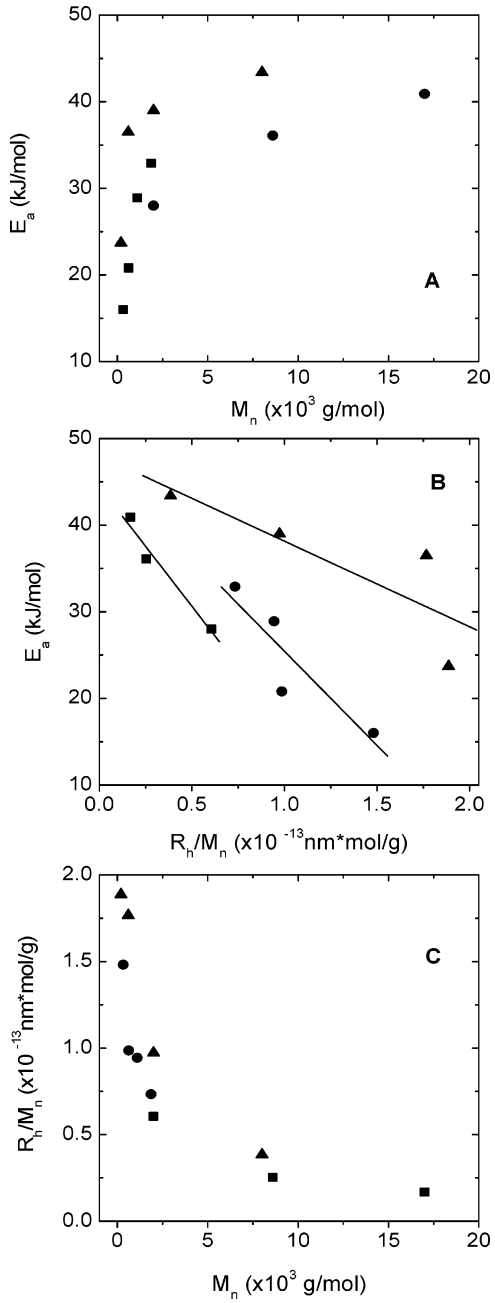

Figure 9. (A) Variation of the apparent activation energy (E_a) obtained from the $k\beta^2$ parameter as a function of the molecular weight (M_n) of the diffusants. (B) Variation of E_a as a function of the ratio of R_h/M_n. (C) Variation of R_h/M_n as a function of M_n of the diffusants. Squares, poly(propylenimine) dendrimers; circles, HBPG-4; triangles, linear PEG. The lines are drawn as visual guides.

volume (or reciprocal density) of the polymer, and it decreases with the molecular weight (Figure 9C). This behavior indicates that the conformation of the diffusants becomes more compact (with higher density) when the molecular weight increases. Figure 9C also shows that, for similar molecular weight, the density of the molecules follows a order from PPI(TEO)$_x$ dendrimers to HBPGs and then to linear PEGs. At a very high density (when R_h/M_n becomes very small), the three kinds of diffusants approach a similar value of apparent activation energy. Extrapolation to R_h/M_n to 0 gives E_a values of 45 ± 2, 47 ± 8, and 48 ± 7 kJ/mol for PPI-(TEO)$_x$ dendrimers, HBPGs, and PEGs, respectively.

Conclusion

It is clearly shown that the self-diffusion coefficients of the HBPG decrease with increasing molecular size of the diffusant, with increasing PVA concentration but with decreasing temperature. These results show that for the same molecular weight and at the same PVA concentration the diffusion is mainly affected by the size of the diffusant resulting from the molecular shape when specific interactions are not predominant. As expected, larger diffusing molecules need higher apparent activation energy to diffuse in the polymer systems. For all diffusants, the density increases with the molecular weight, and for the diffusants with similar molecular weight the density increases from linear PEGs to HBPGs and then to PPI(TEO)$_x$ dendrimers. The qualitative value of the density distribution for the three kinds of diffusants is different. The fractal dimension value ($1/\alpha$) obtained for PPI(TEO)$_x$ dendrimers indicates that the density distributions are close to a compact space-filling structure while the values of HBPGs are similar to those of swollen polymer chains or polymers in good solvent. Furthermore, the density distribution of linear PEGs corresponds to polymer coils in a θ-solvent.

The physical model of Petit et al. describes well the variation of the self-diffusion coefficient with the molecular weight of the HBPG, the polymer concentration, and the temperature. However, the model in its present form does not provide an adequate description of the effects of both size and shape of the diffusants on the self-diffusion coefficient. Molecular weight alone cannot account for the size effect. The shape of the diffusants, and hence the molecular density distribution of the diffusant, should be an important factor to be considered in the diffusion process.

Acknowledgment. The financial support from the Natural Sciences and Engineering Research Council (NSERC) of Canada and the Canada Research Chair Program is gratefully acknowledged. The authors also thank Ms. H. Thérien-Aubin and Dr. C. Malveau for their help in selected NMR experiments.

References and Notes

(1) Bon, C. L.; Nicolai, T.; Kuil, M. E.; Hollander, J. G. *J. Phys. Chem. B* **1999**, *103*, 10294−10299.
(2) Wisnudel, M. B.; Torkelson, J. M. *Macromolecules* **1996**, *29*, 6193−6207.
(3) Gao, P.; Fagerness, P. E. *Pharm. Res.* **1995**, *12*, 955−964.
(4) von Meerwall, E. D. *Adv. Polym. Sci.* **1984**, *54*, 1−29.
(5) Fujita, H. *Adv. Polym. Sci.* **1961**, *3*, 1−47.
(6) Yasuda, H.; Lamaze, C. E.; Ikenberry, L. D. *Makromol. Chem.* **1968**, *118*, 19−35.
(7) Vrentas, J. S.; Duda, J. L. *J. Polym. Sci., Polym. Phys. Ed.* **1977**, *15*, 403−416.
(8) Vrentas, J. S.; Duda, J. L. *J. Polym. Sci., Polym. Phys. Ed.* **1977**, *15*, 417−439.
(9) Phillies, G. D. J. *Macromolecules* **1986**, *19*, 2367−2376.
(10) Vrentas, J. S.; Vrentas, C. M. *Macromolecules* **1994**, *27*, 4684−4690.
(11) Petit, J.-M.; Roux, B.; Zhu, X. X.; Macdonald, P. M. *Macromolecules* **1996**, *29*, 6031−6036.
(12) Amsden, B. *Macromolecules* **1998**, *31*, 8382−8395.
(13) Masaro, L.; Zhu, X. X. *Prog. Polym. Sci.* **1999**, *24*, 731−775.
(14) Storey, R. F.; Mauritz, K. A.; Cox, B. D. *Macromolecules* **1989**, *22*, 289−294.
(15) Mauritz, K. A.; Storey, R. F.; George, S. E. *Macromolecules* **1990**, *23*, 441−450.
(16) Von Meerwall, E. D.; Skowronski, D.; Hariharan, A. *Macromolecules* **1991**, *23*, 2441−2449.
(17) Yu, W.; von Meerwall, E. D. *Macromolecules* **1990**, *23*, 882−889.

(18) Zhu, X. X.; Macdonald, P. M. *Macromolecules* **1992**, *25*, 4345−4351.
(19) Zhu, X. X.; Wang, F.; Nivaggioli, T.; Winnik, M. A.; Macdonald, P. M. *Macromolecules* **1993**, *26*, 6397−6402.
(20) Petit, J.-M.; Zhu, X. X.; Macdonald, P. M. *Macromolecules* **1996**, *29*, 70−76.
(21) Masaro, L.; Zhu, X. X.; Macdonald, P. M. *Macromolecules* **1998**, *31*, 3880−3885.
(22) Masaro, L.; Ousalem, M.; Baille, W. E.; Lessard, D.; Zhu, X. X. *Macromolecules* **1999**, *32*, 4375−4382.
(23) Masaro, L.; Zhu, X. X. *Macromolecules* **1999**, *32*, 5383−5390.
(24) Baille, W. E.; Malveau, C.; Zhu, X. X.; Kim, Y. H.; Ford, W. T. *Macromolecules* **2003**, *36*, 839−847.
(25) Salazar, R.; Fomina, L.; Fomine, S. *Polym. Bull. (Berlin)* **2001**, *47*, 151−158.
(26) Sunder, A.; Hanselmann, R.; Frey, H.; Mülhaupt, R. *Macromolecules* **1999**, *32*, 4240−4246.
(27) Mandal, H.; Hay, A. S. *Polymer* **1997**, *38*, 6267−6271.
(28) Tanner, J. E. *J. Chem. Phys.* **1970**, *52*, 2523−2526.
(29) Callaghan, P. T.; Trotter, C. M.; Jolley, K. W. *J. Magn. Reson.* **1980**, *37*, 247−259.
(30) Stilbs, P. *Prog. Nucl. Magn. Reson. Spectrosc.* **1987**, *19*, 1−45.
(31) Price, W. S. *Concepts Magn. Reson.* **1997**, *9*, 299−336.
(32) Mills, R. *J. Phys. Chem.* **1973**, *77*, 685−688.
(33) Tomlinson, D. J. *Mol. Phys.* **1972**, *25*, 735−738.
(34) Amman, C.; Meier, P.; Merbach, A. E. *J. Magn. Reson.* **1982**, *46*, 319−322.
(35) Pasch, H.; Schrepp, W. *MALDI-TOF Mass Spectrometry of Synthesis Polymers*; Springer-Verlag: Berlin, 2003.
(36) Tokar, R.; Kubisa, P.; Penczek, S. *Macromolecules* **1994**, *27*, 320−322.
(37) Vandenberg, E. J. *J. Polym. Sci., Polym. Chem. Ed.* **1985**, *23*, 951−970.
(38) Frey, H.; Hölter, D. *Acta Polym.* **1999**, *50*, 67−76.
(39) Hanselmann, R.; Hölter, D.; Frey, H. *Macromolecules* **1998**, *31*, 3790−3801.
(40) Waldeck, A. R.; Kuchel, P. W.; Lennon, A. J.; Chapman, B. E. *Prog. Nucl. Magn. Reson. Spectrosc.* **1997**, *30*, 39−68.
(41) Rietveld, I. B.; Bedeaux, D. *Macromolecules* **2000**, *33*, 7912−7917.
(42) Roover, J.; Zhou, L.-L.; Toporowski, P. M.; van der Zwan, M.; Iatrou, H.; Hadjichristidis, N. *Macromolecules* **1993**, *26*, 4324−4331.
(43) Flory, P. J. *Principles of Polymer Chemistry*, Cornell University Press: Ithaca, NY, 1953.
(44) Flory, P. J. *J. Am. Chem. Soc.* **1941**, *63*, 3083, 3091, 3096.
(45) Pickup, S.; Blum, F. D. *Macromolecules* **1989**, *22*, 3961−3968.
(46) Stancik, C. M.; Pople, J. A.; Trollsås, M.; Lindner, P.; Hedrick, J. L.; Gast, A. P. *Macromolecules* **2003**, *36*, 5765−5775.
(47) Scherrenberg, R.; Coussens, B.; Van Vliet, P.; Edouard, G.; Brackman, J.; De Brabander, E. *Macromolecules* **1998**, *31*, 456−461.
(48) Pütz, M.; Kremer, K.; Everaers, R. *Phys. Rev. Lett.* **2000**, *84*, 298−301.
(49) King, S. M. *Modern Techniques for Polymer Characterization*; John Wiley & Sons: New York, 1999.
(50) Geladé, E. T. F.; Goderis, B.; De Koster, C. G.; Meijerink, N.; Van Benthem, R. A. T. M.; Fokkens, R.; Nibbering, N. M. M.; Mortensen, K. *Macromolecules* **2001**, *34*, 3552−3558.
(51) De Gennes, P. G. *Scaling Concepts in Polymer Physics*; Cornell University Press: Ithaca, NY, 1979.
(52) Peppas, N. A.; Lustig, S. R. *Hydrogels in Medicine and Pharmay*; CRC Press: Boca Raton, FL, 1986−1987; Vol. I, Chapter 3.
(53) Schaefer, D. W.; Han, C. C. *Dynamic Light Scattering and Velocimetry: Applications of Photon Correlation Spectroscopy*; Pecora, R., Ed.; Plenum Press: New York, 1982.
(54) Horkay, F.; Burchard, W.; Geissler, E.; Hecht, A.-M. M. *Macromolecules* **1993**, *26*, 1296−1303.
(55) Wang, B.; Mukataka, S.; Kodama, M.; Kokufuta, E. *Langmuir* **1997**, *13*, 6108−6114.
(56) Wang, B.; Mukataka, S.; Kokufuta, E.; Ogiso, M.; Kodama, M. *J. Polym. Sci.* **2000**, *38*, 214−221.
(57) Horkay, F.; Burchard, W.; Geissler, E.; Hecht, A.-M.; M. *Makromol. Chem. Macromol. Symp.* **1993**, *76*, 145−154.
(58) Peppas, N. A. *Hydrogels in Medicine and Pharmay*; CRC Press: Boca Raton, FL, 1986−1987; Vol. II, Chapter 1.

MA049588A